COMPUTATIONAL RESEARCH PROGRESS IN APPLIED SCIENCE & ENGINEERING (CRPASE)

CRPASE: TRANSACTIONS OF CIVIL AND ENVIRONMENTAL ENGINEERING

Journal homepage: http://www.crpase.com

CRPASE: Transactions of Civil and Environmental Engineering 8 (2) Article ID: 2787, 1–6, June 2022 ISSN 2423-4591

Research Article

Seismic Evaluation of the Cheng and Chen Modified Model Using Shear Keys in Steel Beam-to-Concrete Column Connections

Meissam Nazeryan [1*], Mahdi Feizbahr[2]

[1] *Department of Civil Engineering, Sharif University of Technology, Tehran, Iran*
[2] *School of Civil Engineering, Engineering Campus, Universiti Sains Malaysia, 14300 Nibong Tebal, Penang, Malaysia*

Keywords

Steel beam,
Concrete column,
Finite element analysis,
RCS.

Abstract

Frames consisting of composite reinforced concrete and steel (RCS) have been considered as structural systems for several years. This system benefits from the advantages of both systems by optimally combining steel and concrete structural elements. These connections are of two types, which include connections with a through-beam and connections with a through column. In this research, the laboratory model of previous studies has been simulated in ABAQUS finite element software and the seismic performance of RCS joints under cyclic loads and uniform loads was investigated. After validating the finite element model, a parametric study (checking the thickness of the steel panel in the joint area, checking the thickness of the cover sheet, etc.) was performed. Finally, after comparing the results of this type of connection, a modified model was presented which, in addition to increasing the capacity, shows a much more stable and desirable behavior.

1. Introduction

Numerical modeling is a widely economical time-saving applied technique to solve complex problems and it has been widely used in civil engineering problems [1-5]. In recent years, RCS systems, as one of the new building systems consisting of reinforced concrete columns and steel beams, have been widely considered in the design and construction of buildings in the United States and Japan [6, 7]. In Japan large construction companies have developed their facilities and invested in research on RCS systems. As a result, a large number of beam-to-column details have been proposed to implement this system so far [8-10]. These systems are typically based on standards published by the Japan Institute of Architecture [11] and the Japan Building Center (BCJ). 1994) However, most of the new details of these connections are not covered by the standards. Developing basic design methods for RCS systems and connections is an urgent need in Japan. The study of the interconnection of RCS systems included the study of "composite and hybrid structures" as part of a joint US-Japanese seismic research program that began in April 1993 as a five-year research program [12]. Numerous experimental studies have been performed to study the performance of RCS. Sheikh, Deierlein, Yura and Jirsa [13] tested RCS internal connections on a scale of 3.2 at the University of Texas. RCS connections have also been tested by KANNNO [14] at Cornell University. Kim and Noguchi [15] studied the shear strength of RCS joints in detail through finite element analysis. To estimate the shear strength of RCS internal and external joints, experimental research including 9 RCS external joints was performed at the University of Michigan [16, 17].

Cheng and Chen [18] tested six RCS connections by considering different parameters such as Connection stirrups, beam cross-section effects and loading protocol. All

* Corresponding Author: Meissam Nazeryan
E-mail address: Meissam.nazeryan@alum.sharif.edu

Received: 19 February 2022; Revised: 30 March 2022; Accepted: 29 April 2022
https://doi.org/10.52547/crpase.8.2.2787

Academic Editor: **Vahid Najafi Moghadam Gilani**

Please cite this article as: M. Nazeryan, M. Feizbahr, Seismic Evaluation of the Cheng and Chen Modified Model Using Shear Keys in Steel Beam-to-Concrete Column Connections, Computational Research Progress in Applied Science & Engineering, CRPASE: Transactions of Civil and Environmental Engineering 8 (2022) 1–6, Article ID: 2787.

research on this type of composite structure up to 2011 was reviewed by Li, Li, Jiang and Jiang [19]. Noguchi and Uchida [20] investigated two RCS frames focusing on connection failure and investigating connection mechanism states through nonlinear FEM analysis. Li, Li and Jiang [21] proposed a model and conducted a parametric study to investigate the behavior of composite concrete columns by continuous compound spiral ties and enclosed steel beams. Alizadeh, Attari and Kazemi [22] tested two new cases of RCS internal connections based on the strong column weak-beam (SCWB) criterion to study the performance of new details for RCS connections.

Xu, Fan, Lu and Li [23] proposed a new type of pre-pressed spring self-centering energy dissipation system (PS-SCED) that combines friction mechanisms between internal and external pipe components for energy supply. Cao, Feng and Wu [24] studied the seismic performance of reinforced concrete frames (RC) reinforced by steel bracing, which considers the effect of filler walls. Since the implementation of RCS connections of the through-beam is stronger than the connections of the through-column, therefore, in this research, a model will be investigated that in addition to ease of implementation, the resistance of the connection is not less than the connections of the beam type.

2. Experiments by Cheng and Chen [18]

In this study, the seismic behavior of the connection of steel beams to concrete columns without and with the slab in two modes was evaluated at the Earthquake Engineering Research Center (NCREE) in Taiwan. A total of six cross-shaped joints were made and evaluated. All specimens in this experiment have the same dimensions as steel beams with dimensions $H596 \times 199 \times 10 \times 15$ and concrete columns with dimensions $65 \times 65cm$. Based on the combination of available loads, the dimensions of the beams from the roof to the first floor were calculated as H596×199×10×15, H500×200×10×16, and H366 199×7×11, respectively.

Figure 1 describes how to perform the test. Before performing the test, the hydraulic jack applies a constant axial load of 1000 kN to the top of the column, which represents the gravitational load obtained from the frame analysis. Hydraulic actuators on both ends of the beam apply a single cyclic load via triangular displacement (Figure 2). During the test, a horizontal actuator at the top of the column keeps the column in its current position and only allows it to rotate within the plate.

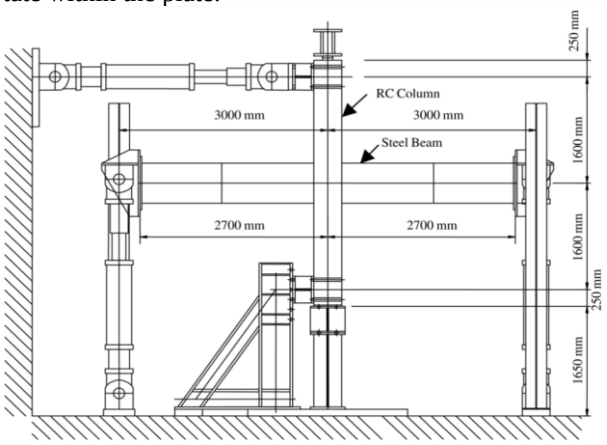

Figure 1. Schematic diagram of the experiment setup

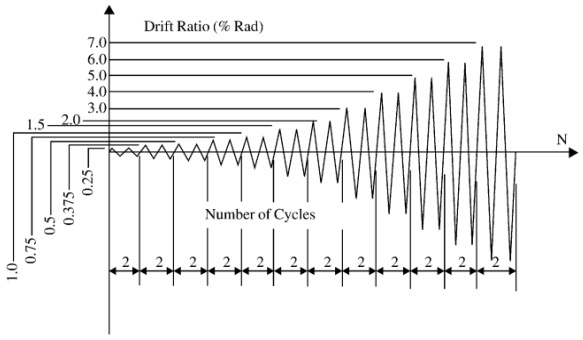

Figure 2. A displacement diagram applied to the end of the beams

2.1. Finite Element Modeling Using ABAQUS Software

ABAQUS software was developed in 1978 by ABAQUS, one of the leading companies in the field of finite element software. In an implicit nonlinear static analysis in this software, two methods of analysis Static General and Static Riks procedure can be used. In this research, the Static General nonlinear analysis method with Newton-Raphson convergence algorithm has been used. The initial increments value for analysis is 0.001, the value of the minimum increment is equal to a small value of 1×10-10, the maximum number of increments per step is 10000 and the selection of increments is selected automatically.

2.1.1. Stress-compressive Strain Curve of Concrete

This diagram is determined based on the results of the uniaxial concrete compression test. For pressurized concrete, three areas of the diagram are introduced. The first part of the diagram is assumed to be elastic. The value of this stress is considered equal to $0.4f_c^{'}$ in which $f_c^{'}$ is the compressive strength of concrete. The strain ε_1 related to the stress is equal to 0.0022. The Young's modulus is also calculated based on [13] and the Poisson ratio is equal to 0.2. The second part of the diagram, which has a parabolic shape, starts from a point with limited stress and continues until it reaches the highest compressive strength of concrete. This part of the graph is determined by Eq. (1)

$$\sigma_c = \left(\frac{kn - n^2}{1 + (k-2)n}\right) f_{ck} \quad (1)$$

in which:

$$\varepsilon_{c1} = 0.0022,\ k = 1.1E_{cm} \times \frac{\varepsilon_{c1}}{f_{ck}},\ n = \frac{\varepsilon_c}{\varepsilon_{c1}} \quad (2)$$

where, Ecm is the concrete modulus of elasticity.

The third part of the stress-strain curve is the descending part of the graph from f_c to rf_c, in which the reduction factor r is considered to be 0.85. The final strain of concrete related to rf_c stress ε_{cu} in rupture is 0.01.

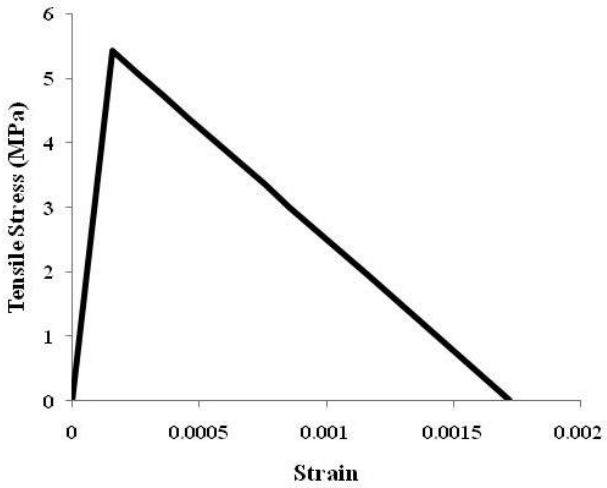

Figure 3. The tensile stress-strain curve for concrete with compressive strength equal to $f_c^{'} = 54MPa$

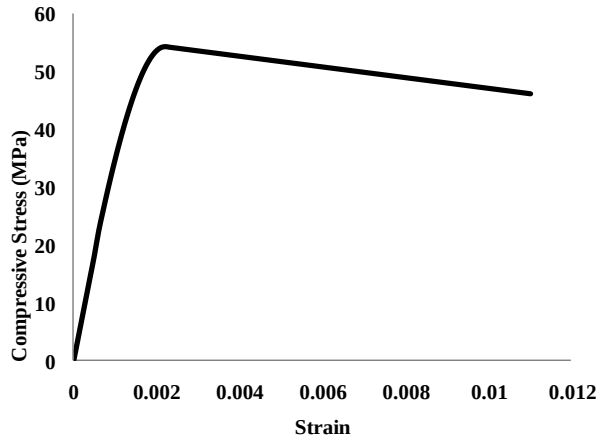

Figure 4. The stress-strain curve for concrete with compressive strength equal to $f_c^{'} = 54MPa$

2.1.2. Steel Materials

The bilinear elastoplastic model was used for steel beams and reinforcements. It was also assumed that the behavior was the same in tension and pressure.

2.1.3. Boundary Conditions

In laboratory tests, the concrete column belongs to the first floor and its connection to the foundation is also involved. Therefore, in simulation, all the degrees of transitional and rotational freedom U_1, U_2, U_3, UR_1, UR_2, UR_3 at the column foot, which is connected to the rigid plane of the support, are closed. This boundary condition is applied to the reference point of the rigid plane, which is affected by the movement of other nodes. In a laboratory test, a hydraulic actuator keeps the column in its current position before the test begins and only allows it to rotate within the plate. In the software, only the degree of freedom UR_2 was left open to simulate the boundary conditions at the top of the column. The beams at both ends can be moved up and down and can only rotate inside the plate. In the finite element model, only the degrees of freedom U_3 and UR_2 were left open at both ends of the beam, but the rest of the degrees of freedom, including U_1, U_2 and UR_1, UR_3 remained closed.

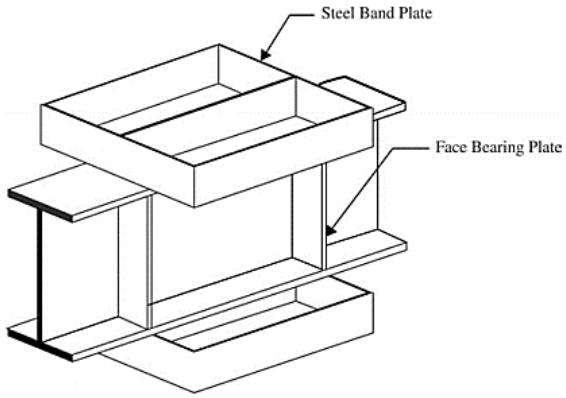

Figure 5. The steel part of the connection includes beams and steel band plate (SBP)

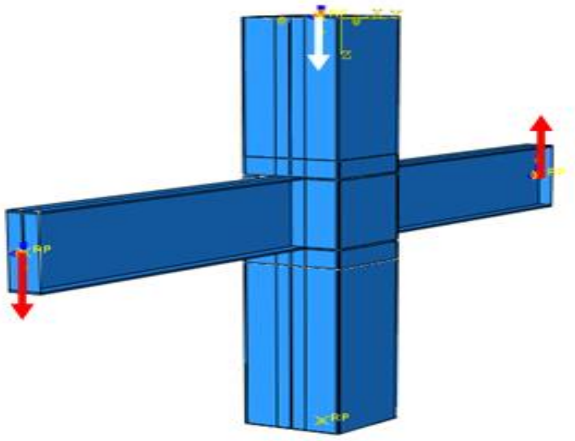

Figure 6. Displacement applied to the end of the beams and the axial load applied to the top of the column in the FE model

2.1.4. Type and size of elements

Concrete columns were simulated with three-dimensional C3D8R elements available in the ABAQUS software library, which is essentially the same 8-point element used for nonlinear analysis involving the interaction of two objects, large deformations, plasticity, and failure. Reinforcements and rigid support plates were also modeled by T3D2 and R3D4 truss elements, respectively. Also, to reduce the analysis time, larger elements were used in most parts and smaller elements were used in the connection areas. The dimensions of the elements in most parts of the beam and column were 35mm, while the smallest of them was considered 18mm.

3. Evaluation of Finite element Analysis Results and Laboratory Results

As can be seen from Figure 7, the results of numerical analysis and laboratory results in low drifts up to less than 4% are consistent with each other and show quite similar behavior and stability, and in drift 4% experience maximum resistance. But in drifts higher than this value, because the behavioral model of steel used in the finite element model has a completely elasto-plastic behavior and no rupture was defined for it, the resistance has not decreased and has reached a constant value up to 7% drift, but the laboratory model has experienced a decrease in resistance in higher cycles after reaching a maximum of 4% resistance in the drift.

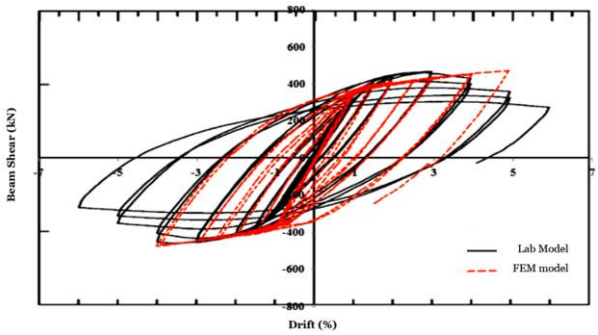

Figure 7. Comparison between beam shear diagram vs end displacement of Laboratory and FEM models

3.1. Distribution of the Minimum Main Stresses of the Connection

The shear strength of the joint is calculated based on the effective width of the concrete joint and is equal to the sum of the inner and outer widths of the panel. The participation of concrete in withstanding the compressive stresses of the connection zone, outside the range of beam wings, depends on the activation of horizontal compression struts, which are formed by crushing double sheets or steel columns on the concrete above and bottom of the joint. External axial pressure at the end of the compression strut is counteracted by the horizontal restraints above and bottom of the beam. The top and bottom restraints of the beam are necessary to counteract the vertical and parallel tensile forces of the beam. The forces perpendicular to the beam are self-balancing and the forces parallel to the beam are transmitted to the external compressive range. In this section, the mechanisms formed in the internal and external concrete joints resulting from the finite element results were shown. Figure 8 clearly shows how these mechanisms are formed.

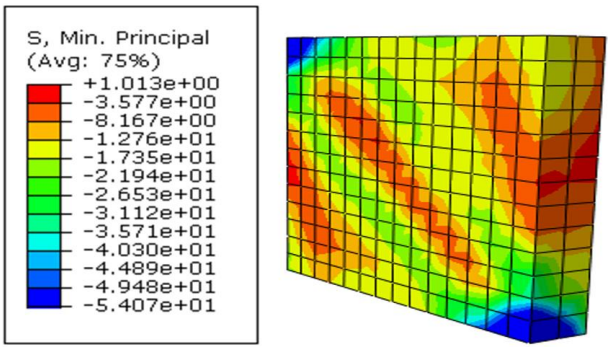

(a)

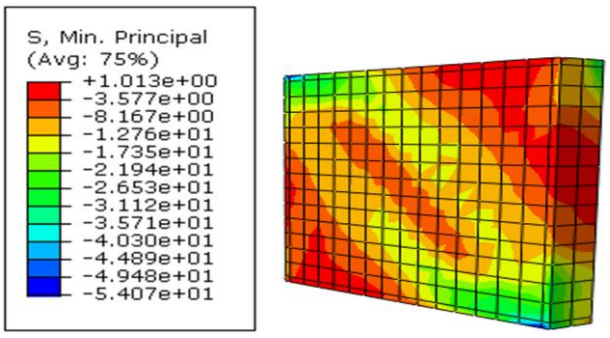

(b)

Figure 8. Formation of diagonal compression struts in: a) Internal concrete panel b) External concrete panel

4. Modified Model

In this study, by modifying the Cheng and Chen [18] model, so that the beam flange are removed in the joint area and by adding the effect of the transverse beam, the through-plate is extended out of the joint and by attaching the beam web and flange to this through-plate according to Figure 15, Beam was connected to the connection. Also, the design of this through-plate was done in such a way that the cross-sectional area of the through-plate was greater than the plastic section of the beam. Based on this, the thickness of the through-plate equal to 20 mm was selected. Also, the effect of the vertical beam on the main axis of the beam was considered by considering the steel panel in the vertical direction. In this way, the connection area was turned into four zones, in each corner of the zone, five rows of L-shaped plates were used according to Figure 9-b. Also, the gaps in the joint area were removed and Steel-Concrete Plate composite (SCP) with a thickness of 15 mm was used instead of steel band plates.

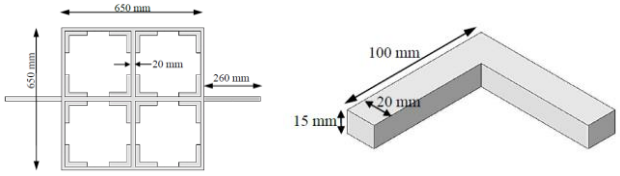

a) steel section properties b) shear keys properties

Figure 9. Cheng and Chen [18] suggested modified model

4.1. Investigation of the Strength of the Suggested Connection in Comparison with the Cheng and Chen model

From the comparison between the results of the Cheng and Chen [18] model and the suggested correction model, it was found that in the whole loading time, the floor shear responses to the floor drift for the suggested model have higher values in terms of hardness and strength. The responses of the finite element models for the Cheng and Chen [18] model and the suggested model with through-plates and shear keys under unilateral loading are also given in Figure 10.

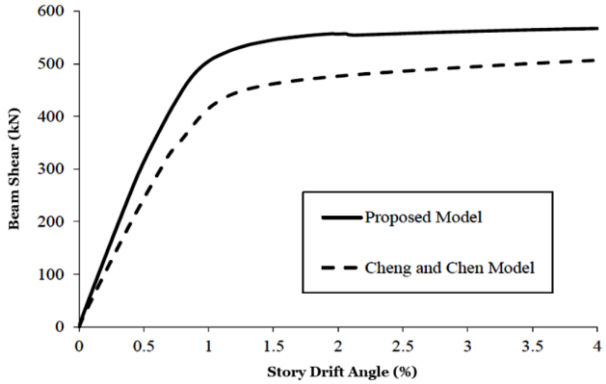

Figure 10. Response of finite element models to uniform loading for Cheng and Chen [18] models and suggested model

4.2. Stress Distribution in the Through-plate and the Shear Keys

Since in the sample tested by Cheng and Chen, a drift equal to 1.4% was considered, in this modified model, this drift was used to examine the mechanisms. at the drift of approximately equal to 1.4 %, the web of steel plate reaches the yielding stress from the middle zone and gradually all the zones reach the yielding stress with increasing the drift. Because in this example the joint area is well reinforced, the stresses in the steel beam core in the middle zone of the joint reach close to the yield point but no plastic joint is formed inside the joint. Figure 11 shows the contour distribution of Von-mises stresses in the steel beam web at the drift equal to1.4%.

4.3. Stress Distribution in the Concrete of the Joint Area

As shown in Figure 12, the concrete in the joint area comes into play against crushing between the shear keys and the SCP. Resistant of the concrete joint area depends on two factors of friction between concrete and steel, which are considered by shear keys. The second factor is SCP, which helps to form a concrete strut in the connection zone and circulation of forces. In this section, the mechanisms formed in the concrete of the joint area, resulting from the results of finite elements, were shown. Figure 12 shows well how this mechanism is formed.

4.4. Mechanism of Plastic Joint Formation

As mentioned earlier, the new connection was designed so that a plastic joint was formed inside, and no part of the connection reached the yield point. This mechanism is desirable because after the beam is plasticized, it is possible to repair and improve the structure. However, if this happens inside the connection, it will be practically impossible to repair and improve the structure. In this new model, after analysis, it was observed that plastic strains were created inside the beam-related elements, which indicates the formation of a plastic joint inside the beams. Of course, in the compression flange, this was accompanied by flange buckling, which is also shown in Figure 13.

4.5. Cracking in the Concrete Column

Considering that in this model similar to the Cheng and Chen [18] test, a displacement is applied to the end of the beams and the column is kept on top of it and only the rotation inside the plate is allowed and it is self-rigid at the other end. Therefore, the amount of rotation is small, which causes very little damage to the column and few cracks in the joint area of the concrete column. Also, transverse cracks occur in the top and bottom of the right part of the steel beam. Figure 14 shows the cracks obtained from the finite element analysis results that are very limited and small.

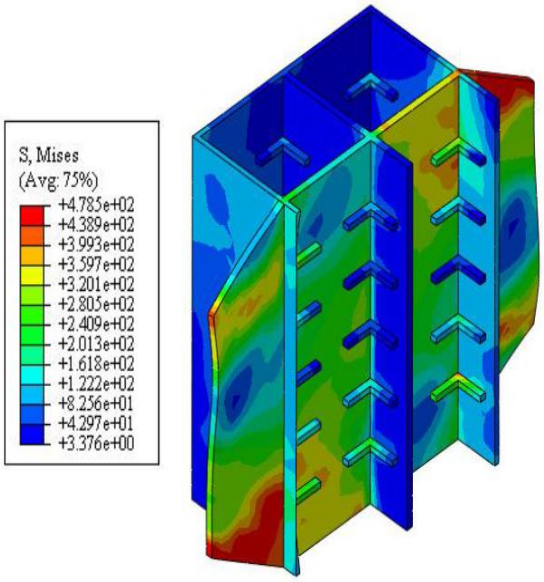

Figure 11. Contour distribution von-mises stresses in the through-plate and the shear keys at the drift of 1.4%

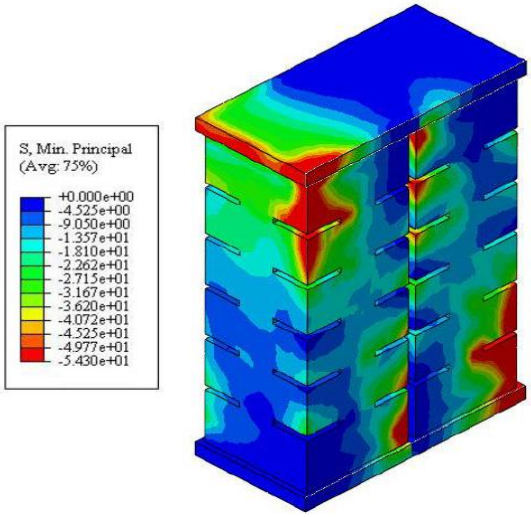

Figure 12. Contour distribution of minimum main stresses in the concrete of the joint zone

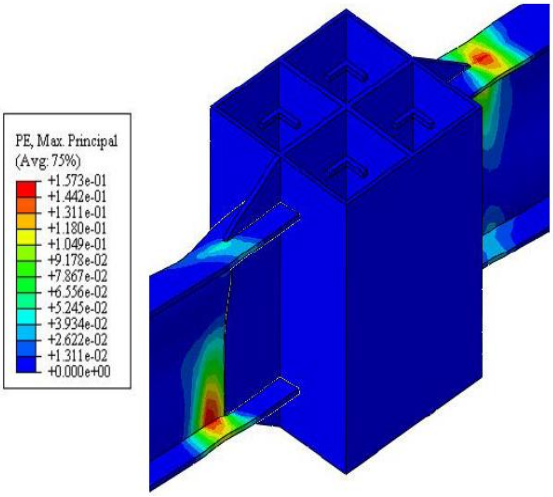

Figure 13. Contour distribution of plastic strain in the steel zone

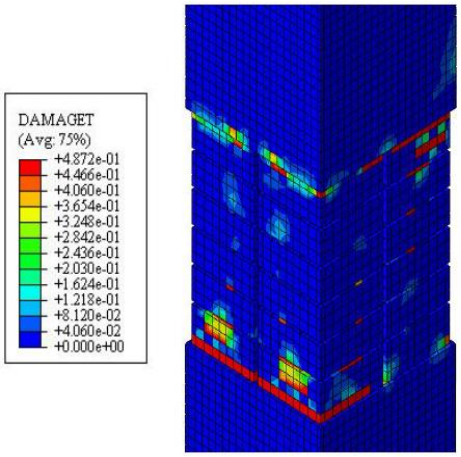

Figure 14. Contour distribution of cracking in concrete

4.6. Contribution of Different Elements of Force in the Connection Zone

The contribution of different elements of the force in the connection zone section which is obtained from the analysis of finite element analysis results by ABAQUS software in the drift of 1.4%, is shown in Table 1.

Tabel 1. Different elements of force Contribution in 1.4% drift

The contribution of through plate	231 KN
The contribution of connection zone concrete	655 KN
Shear capacity of joint	889 KN
The force generated in the concrete strut	1976 KN

5. Conclusion

1. The deformation of the beam and column is obtained from four components, which are: beam bending, column bending, joint crushing and joint panel shear.

2. The joint is divided into three components: shear strength steel panel, inner concrete panel and outer concrete panel. All of these components come into play to withstand shear. First the steel panel yields. After yielding, the shear capacity of the steel web panel slowly increases, then after, the inner and outer concrete panels resist the shear force.

3. The use of a through-plate with shear keys in the joint zone will increase the strength of the joint and the formation of a plastic joint outside the joint and will greatly improve the joint behavior. So that the contribution of concrete in the shear capacity of this area has increased, which was 73% for the modified model of Cheng and Chen.

4. The use of a through-plate for RCS joints converts the forces transmitted from the beam to in-plane stresses and by shear keys, through two shear and support mechanisms, these forces are transferred to the concrete of the joint area and in consequence, these stresses are transferred to the concrete column.

References

[1] H.H. Asli, M. Arabani, Analysis of Strain and Failure of Asphalt Pavement, Computational Research Progress in Applied Science & Engineering 08 (2022) 1–11, Article ID: 2250.

[2] M. Feizbahr, C. Kok Keong, F. Rostami, M. Shahrokhi, Wave energy dissipation using perforated and non perforated piles, International Journal of Engineering 31 (2018) 212–219.

[3] H.H. Asli, A. Hozouri, Non-revenue Water (NRW) and 3D Hierarchical Model For Landslide, Larhyss Journal 48 (2021) 189–210.

[4] K.H. Asli, S.A.O. Aliyev, H.H. Asli, Unaccounted-For Water of a Water System: Some Computational Aspects, Handbook of Research for Fluid and Solid Mechanics: Theory, Simulation, and Experiment, CRC Press (2017) 159–182.

[5] A. Joorabchian, Cold-Formed Steel Stud Assemblies Bearing on Concrete Slabs, (2021).

[6] A. Joorabchian, Z. Li, K.D. Peterman, Experimental and numerical investigation of fixed-height cold-formed steel wall assemblies bearing on concrete slabs, Thin-Walled Structures 166 (2021) 107940.

[7] A. Joorabchian, Z. Li, K.D. Peterman, Numerical investigation of the impact of bearing condition on the axial behavior of variable-height cold-formed steel stud wall assemblies, (2020).

[8] A.I.o.J. (AIJ), Proc., Symp. on Mechanical Behavior of Beam to Column Connections for Composite RCS
Systems, Tokyo, Japan, 1994.

[9] S. Ghods, A. Kheyroddin, M. Nazeryan, S.M. Mirtaheri, M. Gholhaki, Nonlinear behavior of connections in RCS frames with bracing and steel plate shear wall, Steel and Composite Structures 22 (2016) 915–935.

[10] S.M. Mirtaheri, M. Nazeryan, M.K. Bahrani, A. Nooralizadeh, L. Montazerian, M. Naserifard, Local and global buckling condition of all-steel buckling restrained braces, Steel Compos. Struct 23 (2017) 217–228.

[11] A. AIJ, Standards for Structural Calculation of Steel Reinforced Concrete Structures, Architectural Institute of Japan (2001).

[12] H. Yamanouchi, US–Japan cooperative structural research project on composite and hybrid structure. Part 1: Overall research program, Summaries, Technical Papers of Annual Meeting, Architectural Inst., Jpn, (1994) 1521–1522.

[13] T.M. Sheikh, G.G. Deierlein, J.A. Yura, J.O. Jirsa, Beam-column moment connections for composite frames: Part 1, Journal of Structural Engineering 115 (1989) 2858–2876.

[14] R. Kannno, Strength, deformation, and seismic resistance of joints between steel beams and reinforced concrete columns, Doctor Dissertation presented to the Faculty of Graduate School of Cornell University (1993).

[15] K. Kim, H. Noguchi, A study on the ultimate shear strength of connections with RC columns and steel beams, J. Struct. Construct. Eng 507 (1998) 163–169.

[16] G. Parra-Montesinos, J.K. Wight, Seismic response of exterior RC column-to-steel beam connections, Journal of structural engineering 126 (2000) 1113–1121.

[17] G. Parra-Montesinos, J.K. Wight, Modeling shear behavior of hybrid RCS beam-column connections, Journal of Structural Engineering 127 (2001) 3–11.

[18] C.-T. Cheng, C.-C. Chen, Seismic behavior of steel beam and reinforced concrete column connections, Journal of constructional steel research 61 (2005) 587–606.

[19] W. Li, Q.-n. Li, W.-s. Jiang, L. Jiang, Seismic performance of composite reinforced concrete and steel moment frame structures–state-of-the-art, Composites Part B: Engineering 42 (2011) 190–206.

[20] H. Noguchi, K. Uchida, Finite element method analysis of hybrid structural frames with reinforced concrete columns and steel beams, Journal of structural engineering 130 (2004) 328–335.

[21] W. Li, Q.-n. Li, W.-s. Jiang, Parameter study on composite frames consisting of steel beams and reinforced concrete columns, Journal of Constructional Steel Research 77 (2012) 145–162.

[22] S. Alizadeh, N.K. Attari, M. Kazemi, The seismic performance of new detailing for RCS connections, Journal of constructional steel research 91 (2013) 76–88.

[23] L.-H. Xu, X. Fan, D. Lu, Z.-X. Li, Hysteretic behavior studies of self-centering energy dissipation bracing system, Steel and Composite Structures 20 (2016) 1205–1219.

[24] P. Cao, N. Feng, K. Wu, Experimental study on infilled frames strengthened by profiled steel sheet bracing, Steel and Composite Structures 17 (2014) 777–790.